DOI: 10.1002/chem.200701871

A New Nanobiosensor for Glucose with High Sensitivity and Selectivity in Serum Based on Fluorescence Resonance Energy Transfer (FRET) between CdTe Quantum Dots and Au Nanoparticles

Bo Tang,* Lihua Cao, Kehua Xu, Linhai Zhuo, Jiechao Ge, Qingling Li, and Lijuan Yu[a]

Abstract: A novel assembled nanobiosensor QDs-ConA-β-CDs-AuNPs was designed for the direct determination of glucose in serum with high sensitivity and selectivity. The sensing approach is based on fluorescence resonance energy transfer (FRET) between CdTe quantum dots (QDs) as an energy donor and gold nanoparticles (AuNPs) as an energy acceptor. The specific combination of concanavalin A (ConA)-conjugated QDs and thiolated β-cyclodextrins (β-SH-CDs)-modified AuNPs assembles a hyperefficient FRET nanobiosensor. In the presence of glucose, the AuNPs-β-CDs segment of the nanobiosensor is displaced by glucose which competes with β-CDs on the binding sites of ConA, resulting in the fluorescence recovery of the quenched QDs. Experimental results show that the increase in fluorescence intensity is proportional to the concentration of glucose within the range of 0.10–50 μM under the optimized experimental conditions. In addition, the nanobiosensor has high sensitivity with a detection limit as low as 50 nM, and has excellent selectivity for glucose over other sugars and most biological species present in serum. The nanobiosensor was applied directly to determine glucose in normal adult human serum, and the recovery and precision of the method were satisfactory. The unique combination of high sensitivity and good selectivity of this biosensor indicates its potential for the clinical determination of glucose directly and simply in serum, and provides the possibility to detect low levels of glucose in single cells or bacterial cultures. Moreover, the designed nanobiosensor achieves direct detection in biological samples, suggesting the use of nanobiotechnology-based assembled sensors for direct analytical applications in vivo or in vitro.

Keywords: biosensors · conjugation · FRET (fluorescence resonance energy transfer) · glucose · nanotechnology

Introduction

For many decades, scientists have recognized the power of incorporating biological principles and molecules into the design of artificial devices. Biosensors, an amalgamation of signal transducers and biocomponents, play a prominent role in the applied medical fields such as genomics, proteomics, molecular diagnostics, and high-throughput screening.[1] Following recent advances in the growing field of nanotechnology, nanomaterials can be designed as exquisitely sensitive chemical and biological sensors. Nanosensors with immobilized bioreceptor probes that are selective for target analyte molecules are called nanobiosensors and generally consist of a biosensitive part that can either contain biological recognition elements or be made of biological recognition elements covalently attached to the transducer. The interaction between the target analyte and bioreceptor is designed to produce a physicochemical perturbation on the nanobiosensor that can be converted into a measurable effect such as an optical or electrical signal.[2] Thus, the effects of nanomaterials on biological systems as well as research into biomolecules can be realized. Recent advances in the application of nanomaterials as well as their complexes with biomolecules in biosensing and biodetection has attracted great attention. Therefore, the design of elegant assembled nanobiosensors has become an extremely power-

[a] Prof. B. Tang, Dr. L. Cao, K. Xu, L. Zhuo, J. Ge, Q. Li, L. Yu
College of Chemistry
Chemical Engineering and Materials Science
Engineering Research Center of Pesticide and Medicine
Intermediate Clean Production
Ministry of Education
Key Laboratory of Molecular and Nano Probes
Ministry of Education, Shandong Normal University
Jinan 250014 (China)
Fax: (+86) 531-8618-0017
E-mail: tangb@sdnu.edu.cn

Supporting information for this article is available on the WWW under http://www.chemeurj.org/ or from the author.

ful tool for the investigation of direct analysis and detection of biomolecules in vivo or in vitro.

Glucose, as the major energy source in cellular metabolism, plays an important role in the natural growth of cells. Its lack or excess can produce detrimental influence on cellular functions. The glucose level in blood is usually used as a clinical indicator of diabetes,[3,4] and the monitoring of glucose levels in blood with faster and more accurate methods has become an increasingly active area of research.[5–11] Additionally, the monitoring of lower levels of glucose, especially in cell cultures and microbial fermentation processes, is very significant because it could be utilized in high-throughput screening to monitor the response of cells to potential therapeutics and optimize protein biosynthesis.[12,13] Many glucose-assay methods, such as surface plasmon resonance (SPR) spectroscopy,[14,15] fluorescence signal transmission,[13,16–22] and electrochemical signal transduction,[23–27] have been reported. Among these, the widely used commercial glucose test employs electrochemical sensors, and is based on an amperometric electrode at which the glucose concentration is monitored by a change in current flow caused by the enzyme converting glucose into gluconolactone and hydrogen peroxide. However, these sensors are prone to interference from other electroactive species such as ascorbate and ureate in biological systems. In contrast to the electrochemical sensing method, the fluorescence-assay method is selective and nondestructive, and has been extensively used for glucose detection. The technology that has been investigated extensively is based on a competitive binding reaction between the protein concanavalin A (ConA), dextran, and glucose.[14–21] However, these fluorescence-based glucose-assay methods were mostly confined to the millimolar glucose concentration and could not determine directly glucose in biological samples, which restricted their application in cellular signal transduction and protein biosynthesis in single cells or bacterial cultures in which glucose levels are low. Hence, it is desirable to develop a more sensitive and selective, simpler, more stable, and more reliable fluorescence-based method for the direct determination of glucose in biological samples.

In the development of artificial nanobiosensors, fluorescence resonance energy transfer (FRET) has been regarded widely as an extremely useful tool for the sensitive determination of bioactive molecules. Quantum dots (QDs), with their good optical characteristics and high quantum yields of photoluminescence (PL), have been favorably adopted in FRET-based studies for biological analyses and applications.[28–32] As an excellent fluorescent quencher, gold nanoparticles (AuNPs) open new perspectives to detect biomolecules with high sensitivity in FRET systems owing to their high extinction coefficients as well as broad absorption spectrum within the visible light range that overlaps with the emission wavelengths of common energy donors.[33–36] The superiority of QDs-AuNPs donor–acceptor pairs designed as nanobiosensors for biological analyses with high sensitivity has attracted increasing attention. For example, Oh et al.[37] reported an inhibition-assay method for avidin detection with the detection limit of around 10 nM based on the modulation in FRET efficiency between biomolecule-conjugated QDs and AuNPs, respectively. Wang et al.[38] also designed a biosensor to detect avidin with the detected linear range from 0.5 to 370 nM based on FRET between upconversion (UC) nanophosphors and AuNPs. Dyadyusha et al.[39] explored the QDs-AuNPs DNA conjugates as DNA fluorogenic probes for the sensitive detection of single molecule (or low-copy numbers) of DNA in the solution phase. However, the direct practical detection of biomolecules in biological samples has not been realized. Moreover, to the best of our knowledge, no attempt has been made to employ the QDs-AuNPs biocomplex as FRET-based nanobiosensors for monitoring glucose in biological systems. Here, we have designed a new type of assembled FRET-based nanobiosensor QDs-ConA-β-CDs-AuNPs for the direct determination of glucose in human serum. The sensing mechanism is based on the switching off of FRET through the highly specific recognition of ConA by glucose. The nanobiosensor has its merits of very low background signal and high fluorescence recovery in response to glucose, and hence high sensitivity, coupled with excellent selectivity toward glucose over other sugars and most biological species in serum. In addition, the nanobiosensor requires only a small amount (one microliter) of serum sample. Our results demonstrate the value of assembled nanobiosensors for the direct determination of glucose in serum with simplicity and provide the possibility to lower the levels of detectable glucose, especially in single cells or bacterial cultures. Moreover, the designed nanobiosensor uses the QDs-AuNPs biocomplex system to detect glucose directly in practical biological samples, which should facilitate the application of nanobiotechnology-based assembled sensors for direct, practical detection in biological samples.

Results and Discussion

Designing the assembled QDs-ConA-β-CDs-AuNPs glucose nanobiosensor: Our strategy for designing the assembled nanobiosensor for glucose is based on the modulation in FRET efficiency between ConA-conjugated CdTe QDs and β-CDs-modified AuNPs. It is well known that concanavalin A (Con A), a sugar-binding lectin protein with four saccharide binding sites at above pH 7.0, can bind glucose and mannose by means of specific molecular recognition.[40,41] In addition, ConA has been shown to interact with many carbohydrates containing the α-D-glucopyranosyl subunits, such as dextran, glycodendrimer, and biopolymers.[42,43] β-Cyclodextrins (β-CDs), a kind of cyclic oligosaccharide consisting of seven α-D-glucopyranosyl subunits with the characteristics of saccharides, should have affinity with the multivalent ConA protein. Therefore, ConA and thiolated β-cyclodextrins (β-SH-CDs) were selected to modify CdTe QDs and AuNPs, respectively. The specific combination of ConA with β-CDs allows QDs-ConA and AuNPs-β-CDs to be in proximity, and therefore assembles a hyperefficient FRET nano-

biosensor. The mechanism of glucose sensing is outlined in Figure 1. Upon the introduction of glucose into the sensing system, the glucose competes with β-CDs on the binding sites of ConA. This displaces the AuNPs-β-CDs segment of

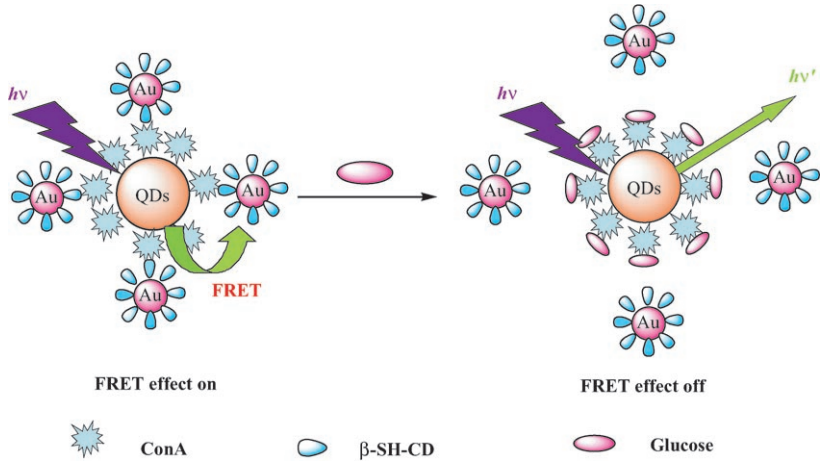

Figure 1. Chemical structure of the QDs-ConA-β-CDs-AuNPs nanobiosensor and schematic illustration of its FRET-based operating principles.

the nanobiosensor and results in the fluorescence recovery of the quenched QDs. The fluorescence increase is related to the concentration of glucose and thus provides a new, simple, and reliable assay of glucose in biological systems such as serum with high sensitivity and good selectivity.

Assembly of the FRET-based nanobiosensor

Formation of β-CDs-modified AuNPs: AuNPs have an extremely high affinity toward thiols and thiol-modified molecules resulting in the intense Au–S covalent bond.[33] Therefore, thiolated β-cyclodextrins (β-SH-CDs) are easily linked with AuNPs. Figure 2 shows the TEM images of the as-synthesized AuNPs (Figure 2a) and β-CDs-modified AuNPs (Figure 2b). The average diameter of the dispersed AuNPs is 13.8±2.0 nm, whereas that of the modified AuNPs increases slightly to 15.7±2.0 nm with a shadow in the edges due to amounts of β-CDs covered with it.

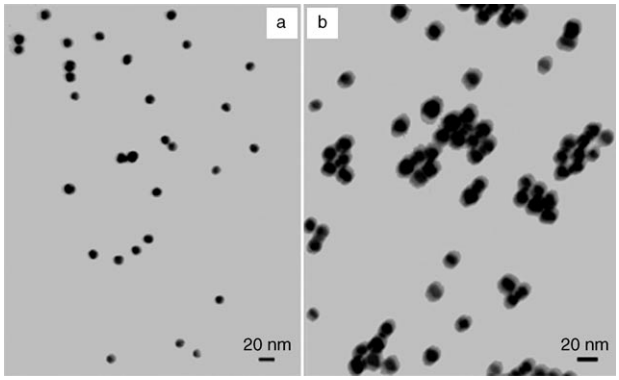

Figure 2. TEM images of a) the as-synthesized AuNPs and b) the β-CDs-modified AuNPs.

In Figure 3a, the IR spectrum of free mono-6-thio-β-CDs shows a peak of S–H stretching mode (≈2550 cm^{-1}), followed by the disappearance of β-CDs-modified AuNPs. Furthermore, the IR spectrum of β-CDs-modified AuNPs (Figure 3b) strongly resembles that of free mono-6-thio-β-CDs, confirming that β-CDs have been modified to AuNPs through the intense covalent bond of Au–S. Additionally, after modification by mono-6-thio-β-CDs, the surface plasmon resonance absorption at 520 nm for AuNPs clearly shifts to 526 nm due to the slight increase in diameter of AuNPs. In addition, there is no significant broadening of the spectrum. This indicates that

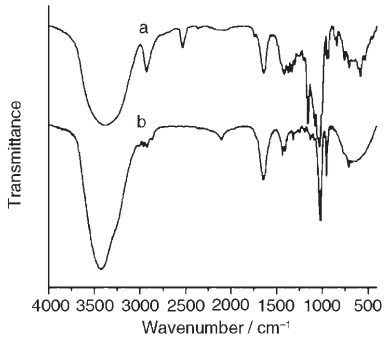

Figure 3. IR spectra of a) mono-6-thio-β-CDs and b) β-CDs-modified AuNPs in a KBr pellet. The modified AuNPs were mixed with KBr and dried under vacuum at 60 °C for pellet preparation.

AuNPs are adequately dispersed after the modification. The phenomena above provide evidence for the strong attachment of β-SH-CDs to AuNPs.

Formation of purified QDs-ConA bioconjugates: The formation of QDs-ConA bioconjugates is confirmed by optical absorption spectra and fluorescence spectra. As shown in Figure 4, after conjugation with ConA, the two absorption peaks of QDs broaden and the maximum fluorescence emission peak red-shifts from 525 to 530 nm, attributable to the increase in the final size of the QDs-ConA bioconjugates formed by the surface modification of QDs.

Figure 5 shows the electropherograms of purified QDs-ConA bioconjugates and free QDs by capillary electrophoresis obtained with a UV-visible detector at 280 and 485 nm, respectively. Our results prove that ultrafiltration is an effective and simple approach to purify QDs-ConA bioconju-

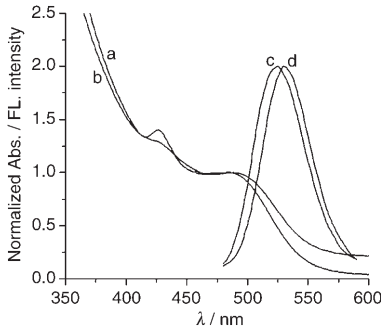

Figure 4. Normalized optical absorption spectra and fluorescence spectra obtained from CdTe QDs (a and c) and QDs-ConA bioconjugates (b and d). Solutions were prepared in PBS buffer (10 mM, pH 7.4).

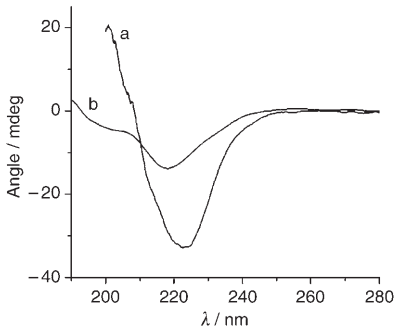

Figure 6. CD spectra of ConA a) before and b) after the conjugation of CdTe QDs. Samples were dissolved in PBS buffer solution (10 mM, pH 7.4). The initial concentration of ConA solution is 1.0 mg mL^{-1}.

gates. As can be seen from Figure 5, the single peak in (a) represents the characteristic peak of free QDs that is detected at wavelength 485 nm. When the capillary electrophoresis was performed with the purified QDs-ConA bioconjugates at wavelengths 485 and 280 nm, respectively, under the same conditions as for free QDs, the single characteristic peak of QDs-ConA bioconjugates appeared. The difference between (b) and (c) in Figure 5 is the intensity of the two peaks, whereas the migration time is consistent, which is due to the different optical absorption intensities of QDs-ConA bioconjugates at 485 and 280 nm. In addition, the single peak that appeared in purified QDs-ConA bioconjugates at 280 nm demonstrates that excess ConA is removed completely during the process of conjugation; the dissociative ConA protein has a strong absorption peak at 280 nm. The different migration times of free QDs and QDs-ConA bioconjugates are due to the change in surface charges on QDs after conjugation with ConA. Therefore, QDs-ConA bioconjugates are purified well through ultrafiltration and excess ConA is removed completely.

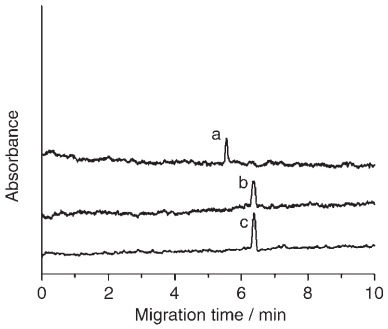

Figure 5. Electropherograms of QDs-ConA bioconjugates and free QDs obtained by capillary electrophoresis: a) free QDs (485 nm, 0.10 mg mL^{-1}); b) QDs-ConA bioconjugates (485 nm, 0.10 mg mL^{-1}); c) QDs-ConA bioconjugates (280 nm, 0.10 mg mL^{-1}).

Biological activity of QDs-ConA bioconjugates: As can be seen from Figure 6, the circular dichroism (CD) spectra of ConA and QDs-ConA bioconjugates are very similar to each other. The small disturbance in the ConA conformation is manifested as a shift in CD spectra minimum from 222 to 217 nm.[44] In addition, compared with the free ConA, the CD spectral peak of QDs-ConA is weaker because of the removal of excess ConA in the conjugation. These results show that the biological activity of ConA does not change during the conjugation process, and ultrafiltration is a valid way to purify QDs-ConA bioconjugates. The CD spectra reveal that the tertiary structure of the ConA remains mostly intact after conjugation.

Confirmation of the FRET mechanism of QDs-ConA and AuNPs-β-CDs

Binding studies of ConA and β-CDs: To study the binding interaction of ConA and β-CDs, we first investigated AuNPs-β-CDs after the addition of ConA and glucose in turn. This were characterized by optical absorption spectra and TEM, as shown in Figures 7 and 8, respectively. As can be seen from Figure 7, AuNPs modified with β-CDs exhibit the surface plasmon resonance peak at 526 nm. After introducing ConA into the AuNPs-β-CDs solution, a significant red-shift to 530 nm and broadening of the absorption peak are observed. This is caused by the aggregation of colloidal AuNPs-β-CDs. Afterwards, the addition of glucose to the above solutions induces competitive dissociation of the ConA protein from β-CDs, and this dissociation is reflected in a shift back to the original spectrum of AuNPs-β-CDs.

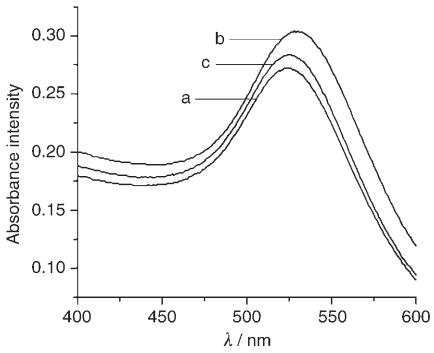

Figure 7. Optical absorption spectra of a = AuNPs-β-CDs showing effects of association with b) ConA and c) dissociation by glucose.

Furthermore, a concomitant narrowing of the optical absorption spectrum is associated with the blue-shift, which is a strong indication of competitive dissociation of ConA from AuNPs-β-CDs. The results reveal that the binding interaction of ConA and β-CDs by means of specific biomolecular recognition is reversible. Moreover, the changes in absorbance intensity are also observed in Figure 7. The addition of ConA induces aggregation of AuNPs-β-CDs and increased absorbance. After dissociation by the addition of glucose solution, the absorbance intensity decreases, but is still slightly higher than the initial intensity before binding of ConA. This indicates that the glucose does not dissociate the ConA and β-CDs complexes completely, which is also confirmed by the slightly more broadened absorbance spectrum of AuNPs-β-CDs. This phenomenon may indicate the nonspecific adsorption of nanoparticles.

Further confirmation of the binding between ConA and β-CDs is provided by the TEM images. Figure 8 shows the micrographs of AuNPs-β-CDs material before and after addition of ConA and glucose in turn. AuNPs-β-CDs appear aggregated rather than being evenly dispersed after interacting with ConA. This is the result of the specific biomolecular recognition occurring between the multivalent protein ConA and the glucopyranosyl groups in β-CDs. In contrast, addition of glucose dissociates the combination of ConA and β-CDs, and thus the dispersed AuNPs-β-CDs appear again. Thus, we can conclude that ConA molecules can easily combine with β-CDs through the multivalent combination sites and this interaction is reversible upon addition of glucose, which displays higher specific recognition of ConA.

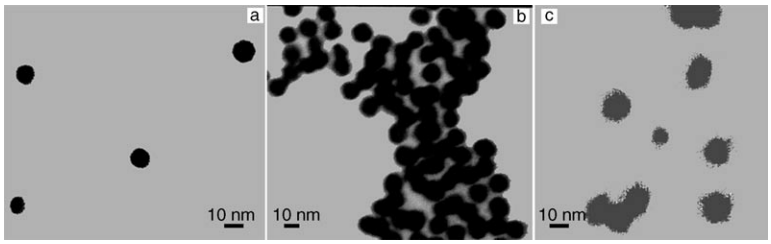

Figure 8. TEM images of a) AuNPs-β-CDs, b) AuNPs-β-CDs after interaction with ConA, c) solution in (b) following addition of glucose.

Stern–Volmer plot: According to the theory of FRET, when the absorption spectrum of the energy acceptor overlaps significantly the fluorescence emission spectrum of the energy donor and when the donor and acceptor are close enough, the emission of the energy donor will be quenched by the acceptor. In our sensing system, the optical absorption spectrum of AuNPs-β-CDs overlaps the fluorescence emission spectrum of QDs-ConA bioconjugates, as illustrated by the above spectral characterization. In addition, the distance between the two relevant saccharide binding sites within the ConA tetramer ($M_w = 104$ kDa) is estimated to be 65 Å.[45] Thus, the binding of ConA and β-CDs brings AuNPs sufficiently close to QDs within the distance range of FRET. It has been reported recently that QDs and AuNPs can be used as an energy donors and acceptors, respectively, in FRET systems by means of specific biomolecular recognition such as avidin–biotin.[37,38] Thereby we can deduce that the interaction of ConA with β-CDs is also analogous to an antigen–antibody reaction. Thus, it is intrinsically possible to couple QDs-ConA with AuNPs-β-CDs to assemble a new FRET nanobiosensor. In our experiments, in order to decrease or avoid the self-absorbance of AuNPs and the nonspecific adsorption of nanoparticles, the modified molecules including ConA and β-CDs were added in excess so that they can wrap up the nanoparticles completely. Thus, the hyperefficient FRET can occur between the donor–acceptor pair, which is illustrated by the well-known Stern–Volmer equation.

When the concentration of QDs-ConA was stabilized at 0.2×, and the content of AuNPs-β-CDs varied from 0–1.2 nM (or 1.2×), we observed a regular decrease in the fluorescence intensity of QDs-ConA. Fluorescence quenching is described by the well-known Stern–Volmer equation:[46] $F_0/F = 1 + K_{SV}$ [AuNPs-β-CDs]. F_0 and F denote the steady-state fluorescence intensities in the absence and presence of the quencher AuNPs-β-CDs, respectively. A plot of F_0/F versus [AuNPs-β-CDs] produced a straight line, as shown in Figure 9, the slope of which gave the Stern–Volmer quenching constant ($K_{SV} = 5.8 \times 10^9\ M^{-1}$).

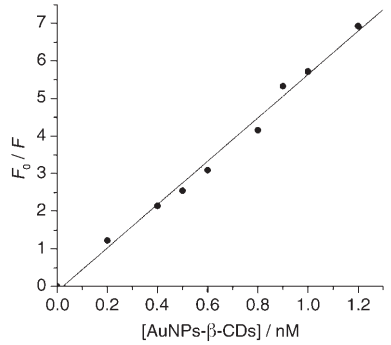

Figure 9. Stern–Volmer plot of F_0/F versus [AuNPs-β-CDs]. The linear approximation gives $F_0/F = -0.13 + 5.8$ [AuNPs-β-CDs], $R = 0.9955$.

Performance characteristics and statistical analysis: In order to further enhance the performance of the assembled nanobiosensor for glucose, we optimized the experimental conditions including the pH of the solution, the volume ratio between AuNPs-β-CDs and QDs-ConA, amounts of the sensing solution, concentration of PBS buffer solution, and time

response of the assay (see Supporting Information). Under optimal conditions, we monitored changes in fluorescence spectra of QDs-ConA-β-CDs-AuNPs in the presence of different concentrations of glucose, as shown in Figure 10. As

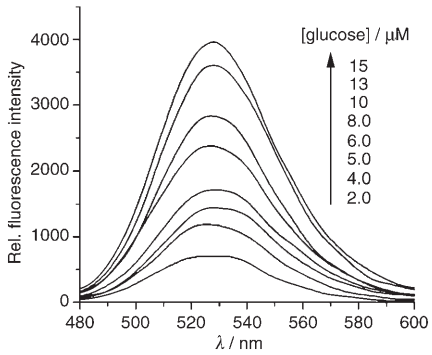

Figure 10. Changes in fluorescence spectra of the nanobiosensor in the presence of different concentrations of glucose under optimal experimental conditions.

expected, there is low background fluorescence signal before addition of glucose due to the high quenching efficiency of AuNPs-β-CDs. Upon the introduction of glucose into the sensing system, glucose occupies competitively the combination sites on ConA, which are originally combined with β-CDs, followed by the restoration of fluorescence of the quenched QDs. In response to glucose assays, the maximum efficiency of fluorescence recovery can reach approximately 90%, which can be calculated from experimental results. As the concentration of glucose increases gradually within the micromolar range, the increase in fluorescence intensity is proportional to the concentration of glucose. A calibration curve of fluorescence signal versus concentration of glucose is observed (Figure 11). Statistical analysis reveals a detection limit of glucose concentration as low as 50 nM. The precision expressed as the relative standard deviation (%RSD), obtained from a series of 11 standard samples each containing 10 μM of glucose, is 2.3. Therefore, the new assembled nanobiosensor designed for the sensitive detection of glucose is feasible and may be applied to the determination of glucose in biological samples.

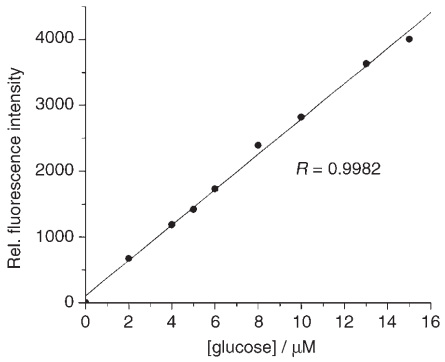

Figure 11. Linear plot of relative fluorescence intensity as a function of glucose concentration.

Effects of sugars and various biological species on the nanobiosensor: To assess the selectivity of the assembled nanobiosensor for glucose, the effects of sugars and common species present in biological systems, especially in serum, on the determination of glucose were examined. An error of ±5.0% in the relative fluorescence intensity is considered tolerable. In the process of determination, 10 μM of glucose was added to each sample and the other interferential species was added subsequently. The concentration of the sugars was 1000-fold that of glucose and these biological species are at normal serum concentrations. Moreover, the normal concentration of glucose in vivo is at the millimolar level, and the detecting concentration range using our proposed method is in the micromolar range. Thus, the designed nanobiosensor can be used to determine glucose in a small amount of serum samples (one microliter) and most interferential species present in serum can not influence glucose determination. Table 1 shows that the relative error of

Table 1. Interferences of various coexisting biological species.

Coexisting substance	Concentration [mol L^{-1}]	Relative error [%]
sucrose	1.0×10^{-2}	2.2
D-fructose	1.0×10^{-2}	0.87
lactose	1.0×10^{-2}	4.8
maltose	1.0×10^{-2}	4.9
mannitol	1.0×10^{-4}	3.5
K^+	2.0×10^{-3}	−3.2
Na^+	1.6×10^{-3}	−3.0
Ca^{2+}	1.4×10^{-2}	0.55
Mg^{2+}	2.9×10^{-4}	−4.2
Ba^{2+}	2.0×10^{-3}	−3.2
Al^{3+}	5.0×10^{-5}	0.49
Cu^{2+}	1.5×10^{-6}	0.51
Zn^{2+}	5.0×10^{-5}	−1.2
Co^{2+}	5.0×10^{-6}	5.1
Fe^{3+}	2.0×10^{-6}	5.4
uric acid	7.2×10^{-6}	4.2
bilirubin	1.0×10^{-6}	4.8
glycine	1.0×10^{-5}	−1.2
arginine	1.0×10^{-5}	−0.35
L-phenylalanine	1.0×10^{-5}	6.1
lysine	1.0×10^{-5}	3.1
L-cystenine	3.6×10^{-5}	4.3
tyrosine	5.0×10^{-5}	−5.5
ascorbic acid	1.0×10^{-5}	3.3
cholesterol	1.0×10^{-5}	3.5

most species is within the range of ±5.0%. Therefore, the assembled nanobiosensor has high selectivity for glucose and can be used for the following direct practical determination in serum samples.

Determination of glucose directly in serum samples and accuracy assessment by recovery experiments: To evaluate the applicability of the assembled nanobiosensor, fluorescence determination in serum samples was performed according to the described procedures. The detected glucose content in serum samples was derived from the standard curve and the regression equation. The average recovery test was performed by using the standard addition method and RSD was generally good, as obtained from a series of six serum

samples. Compared to the certified data obtained by using the Automatic Biochemistry Analyzer (OLYMPUS 5400, Japan), our analytical data summarized in Table 2 indicate that the recovery and precision of the method applied to determine glucose directly in serum samples are satisfactory. Therefore, the newly designed nanobiosensor provides a simple and convenient way to determine glucose content directly with only a microliter amount of serum samples.

Table 2. Analytical results of the direct determination of glucose in serum samples.

Sample	Measured[a] [mM]	Added [mM]	Recovered[a] [mM]	RSD [%, $n=6$]	Recovery [%]	Certified [mM]
1	3.63	3.00	6.76	2.1	104	3.68
2	3.70	3.00	6.75	2.4	102	3.78
3	3.65	3.00	6.56	1.9	97.0	3.68

[a] Mean value of six determinations by the proposed method.

Conclusion

We have described the assembling, properties, and applications of the QDs-ConA-β-CDs-AuNPs, a new nanobiosensor designed based on the FRET mechanism for determining glucose directly with high sensitivity and selectivity in serum samples. The high quantum yields of photoluminescence of QDs, high extinction coefficients of AuNPs, and the specific recognition by ConA of glucose over β-CDs ensure a hyperefficient FRET nanobiosensor system and enhance the sensitivity of the determination. The nanobiosensor features excellent selectivity toward glucose over other sugars and most biological species present in serum, and has a detection limit as low as 50 nM. The results obtained for the direct determination of glucose in normal adult serum samples are in accordance with the analytical method widely used in clinical practice. Therefore, our newly assembled nanobiosensor QDs-ConA-β-CDs-AuNPs provides a simple, sensitive, and selective means to determine directly glucose levels in a small amount of serum in a clinical context and provides the possibility to detect low levels of glucose in single cells or bacterial cultures. Moreover, the designed nanobiosensor enables the direct detection in practical biological samples by means of the QDs-AuNPs biocomplex system, and therefore proposes nanobiotechnology-based assembled sensors for direct analytical applications in vivo or in vitro.

Experimental Section

Materials: Concanavalin A (ConA, type IV), thioglycolic acid (TGA), 1-ethyl-3-(3-dimethylaminopropyl)-carbodiimide (EDC), N-hydroxysuccinimide (NHS) were obtained from Sigma. D-Glucose was purchased from Amresco Corporation. Hydrogen tetrachloroaurate (III) ($HAuCl_4 \cdot 3H_2O$), tellurium powder (99%), sodium hydrogen boride (99%), and β-cyclodextrins (β-CDs) were obtained from China Medicine Group Shanghai Chemical Reagent Corporation. Ultrapure water used in the experiment was purified with the Mill-Q (electric resistivity 18.2 $M\Omega cm^{-1}$) water-purification system. 100k Nanosep filter (Pall Corporation, USA) and Micoron YM-30-30000 NMWL (Millipore, USA) were used as the ultrapurification instrumentation.

Physical instrumentation and methods: Optical absorption spectroscopy measurements were performed by using a UV-1901 PC dual-beam spectrophotometer (Shimadzu Corp. Kyoto, Japan) using 1.0-cm path-length quartz cuvettes. Fluorimetric spectra were obtained by using an Edinburgh FLS920 spectrofluorimeter (Edinburgh Instruments Ltd, England) equipped with a xenon lamp and a quartz cuvette (1.0 cm optical path) as the container. Spectrometer slits were set for 2.0 nm. Transmission electron microscopy (TEM) images were obtained by using a Hitachi Model H-800 instrument (Japan). Infrared spectra were obtained by using a PE-983G IR-spectrophotometer (Perkin–Elmer). Circular dichroism spectra were obtained by using a Circular Dichroism Spectrometer (J-810, JASCO Co., Japan). A JASCO cell of path length 0.10 cm was used. Centrifugation was performed by using a Sigma 3K 15 centrifuge. Capillary electrophoresis was performed by using a QL-1000 instrument with UV/Vis detector (Shandong Normal University). Experimental conditions: capillary with 50 cm effective (55 cm total) length and 75 μm ID. $Na_2B_4O_7$ solution (25 mM, pH 7.4) was used as running buffer. Applied voltage was 12 kV and samples were injected by using pressure at 10 cm psi for 8 s.

Preparation of water-soluble CdTe quantum dots (QDs) and their purification: CdTe QDs were prepared by using the reaction between Cd^{2+} and NaHTe solution in the presence of thioglycolic acid (TGA) as a stabilizer, according to literature.[47] To remove excess thioglycolic acid, the as-prepared QDs were precipitated with an equivalent amount of 2-propanol, and then redispersed in ultrapure water and precipitated with 2-propanol twice. The pellet of purified QDs was dried overnight at RT in vacuum, and the final product in the powder form could be redissolved in ultrapure water (100 mL). The aggregated nanoparticles that appeared in the process of redissolving were removed by ultrafiltration using 100k Nanosep filter under centrifugation (12000 rpm, 5 min). The upper phase was discarded leaving the obtained homogeneous QDs in lower phase as the stock solution. We denote the concentration of purified QDs solution to be 1×.

Preparation of QDs-ConA bioconjugates: ConA was dissolved in phosphate buffered saline solution (PBS, 10 mM, pH 7.4) augmented with $CaCl_2$ (1.0 mM) and $MnCl_2$ (1.0 mM) to obtain a solution (1.0 mg mL^{-1}) that was stored at 4°C. The conjugation involves 1-ethyl-3-(3-dimethylaminopropyl)-carbodiimide (EDC) and N-hydroxysuccinimide (NHS) to form active esters to conjugate the carboxyl groups of QDs to the primary amine groups of ConA. Briefly, EDC (0.50 mg) and NHS (0.25 mg) were added to the stock QDs solution (1.00 mL) to activate QDs in PBS buffer (10 mM, pH 7.4) and incubated for 30 min at RT with continuous gentle mixing. Next, the activated QDs and ConA solution (0.50 mL) were incubated at RT for another 2 h with continuous gentle mixing, and then stored at 4°C overnight. The ConA-conjugated QDs were separated from the solution by removing free ConA as well as other small molecules by ultrafiltration under centrifugation (12000 rpm, 5 min) with YM-30K ultrafilter. The final concentrated QDs-ConA was diluted to 1.00 mL with ultrapure water to give the fixed concentration (1×) ready to use in the following fluorescence assays. The obtained QDs-ConA bioconjugates were characterized by capillary electrophoresis, circular dichroism spectra, UV/Vis absorption spectra, and fluorescence spectra.

Preparation of β-CDs-modified AuNPs: The mono-6-thio-β-CDs were synthesized as previously documented.[48] The mono-dispersed AuNPs with the diameter of about 15 nm were prepared by using the classical citrate reduction route pioneered by Frens.[49] The concentration of the as-prepared AuNPs was calculated to be approximately 1.8×10^{15} particles/L, ≈3.0 nM.[33] Similar to the report by Liu, mono-6-thio-β-CDs (20 mg) was added to the previously prepared AuNPs solutions (50 mL)

under ultrasonic conditions for 10 min and stirred in the dark for another 48 h. Next, unbound mono-6-thio-β-CDs was removed by repeated centrifugation (12000 rpm, 10 min) with DMSO/CH_3CN (v/v = 1:1), followed by redispersing the red precipitate in ultrapure water (50 mL) to get the β-CDs-modified AuNPs. At this stage, complete removal of free mono-6-thio-β-CDs was verified by TLC (silica gel, CH_3CO_2Et/*n*PrOH/H_2O 7:7:5). The β-CDs-modified AuNPs (AuNPs-β-CDs) were characterized by IR and UV/Vis absorption spectroscopy as well as by transmission electron microscopy (TEM). The final concentration of AuNPs-β-CDs was calculated to be approximately 2.0 nM according to the intensity of the absorption spectrum. Please note that we denote the concentration of the as-prepared AuNPs-β-CDs solution to be 2×.

Glucose sensing by fluorescence detection: AuNPs-β-CDs solution (2.00 mL) was added to the prepared QDs-ConA aqueous solution (1.00 mL) for an equilibration period (1 h) to react completely. Under this condition, the nanobiosensor QDs-ConA-β-CDs-AuNPs solution was formed and could be used for the subsequent glucose sensing. Afterwards, the above sensing solution (450 μL), PBS buffer solution (100 μL, 10 mM pH 7.4), and different concentrations of glucose were added to the colorimetric tube (1.50 mL), respectively, and each sample solution was diluted with ultrapure water to a final volume of 1.00 mL. After reaction for 15 min at RT, the fluorescence spectra were obtained within the spectral range of 480 to 600 nm by use of the maximal excitation wavelength at 320 nm. Selectivity experiments were operated according to the same fluorescent detection method.

Glucose detection in serum: The serum samples were obtained by centrifuging (1000 rpm, 5 min) the fresh blood samples (provided by ShengLi hospital of Shandong province, China), which separated cells from all other material. A volume of 1μL of serum sample was subjected to the determination system described and this was followed by fluorescence detection.

Acknowledgements

The authors gratefully acknowledge the financial support from the National Basic Research Program of China (973 Program, 2007CB936000), National Natural Science Funds for Distinguished Young Scholar (No. 20725518), Major Program of National Natural Science Foundation of China (No. 90713019), National Natural Science Foundation of China (20475034), Important Project of Natural Science Foundation of Shandong Province (No. Z2006B09), and the Foundation of State Key Laboratory of Electroanalytical Chemistry.

[1] K. K. Jain, *Clin. Chim. Acta* **2005**, *358*, 37–54.
[2] T. Vo-Dinh, P. Kasili, M. Wabuyele, *Nanomedicine* **2006**, *2*, 22–30.
[3] The Diabetes Control and Complications Trial Research Group, *New Engl. J. Med.* **1993**, *329*, 977–986.
[4] The Diabetes Control and Complications Trial Research Group, *Diabetes* **1997**, *46*, 271–286.
[5] J. S. Schultz, S. Mansouri, I. J. Goldstein, *Diabetes Care* **1982**, *5*, 245–253.
[6] I. Amato, *Science* **1992**, *258*, 892–893.
[7] J. Pickup, L. McCartney, O. Rolinski, D. Birth, *Br. Med. J.* **1999**, *319*, 1289–1292.
[8] T. Koschinsky, L. Heinemann, *Diabetes Metab. Res. Rev.* **2001**, *17*, 113–123.
[9] E. A. Moschou, B. V. Sharma, S. K. Deo, S. Daunert, *J. Fluoresc.* **2004**, *14*, 535–547.
[10] M. Ben-Moshe, V. L. Alexeev, S. A. Asher, *Anal. Chem.* **2006**, *78*, 5149–5157.
[11] T. Zhang, E. V. Anslyn, *Org. Lett.* **2007**, *9*, 1627–1629.
[12] M.-C. Lee, S. Kabilan, A. Hussain, X. Yang, J. Blyth, C. R. Lowe, *Anal. Chem.* **2004**, *76*, 5748–5755.
[13] X.-D. Ge, L. Tolosa, G. Rao, *Anal. Chem.* **2004**, *76*, 1403–1410.
[14] B. Lee, V. H. Perez-Luna, *Anal. Chem.* **2005**, *77*, 7204–7211.
[15] K. Aslan, J. R. Lakowicz, C. D. Geddes, *Anal. Chem.* **2005**, *77*, 2007–2014.
[16] D. L. Meadows, J. S. Schultz, *Talanta* **1988**, *35*, 145–150.
[17] D. L. Meadows, J. S. Schultz, *Anal. Chim. Acta* **1993**, *280*, 21–30.
[18] G. Blagoi, N. Rosenzweig, Z. Rosenzweig, *Anal. Chem.* **2005**, *77*, 393–399.
[19] R. J. Russell, M. V. Pishko, *Anal. Chem.* **1999**, *71*, 3126–3132.
[20] P. W. Barone, R. S. Parker, M. S. Strano, *Anal. Chem.* **2005**, *77*, 7556–7562.
[21] R. Ballerstadt, J. S. Schultz, *Anal. Chem.* **2000**, *72*, 4185–4192.
[22] B. L. Ibey, H. T. Beier, R. M. Rounds, G. L. Cote, *Anal. Chem.* **2005**, *77*, 7039–7046.
[23] W. Chen, H. Yao, C. H. Tzang, J. Zhu, M. Yang, S.-T. Lee, *Appl. Phys. Lett.* **2006**, *88*, 213104.
[24] T. Chen, K. A. Friedman, I. Lei, A. Heller, *Anal. Chem.* **2000**, *72*, 3757–3763.
[25] A. G. Sapre, A. Bedekar, A. V. Deshpande, A. M. Lali, *Biotechnol. Lett.* **2000**, *22*, 569–573.
[26] Y. Tatsu, K. Yamashita, M. Yamaguchi, S. Yamamura, H. Yamamoto, S. Yoshikawa, *Chem. Lett.* **1992**, *8*, 1615–1618.
[27] B. Wang, B. Li, Q. Deng, S. Dong, *Anal. Chem.* **1998**, *70*, 3170–3174.
[28] I. L. Medintz, A. R. Clapp, H. Mattoussi, E. R. Goldman, B. Fisher, J. M. Mauro, *Nat. Mater.* **2003**, *2*, 630–638.
[29] E. R. Goldman, I. L. Medintz, J. L. Whitley, A. Hayhurst, A. R. Clapp, H. T. Uyeda, J. R. Deschamps, M. E. Lassman, H. Mattoussi, *J. Am. Chem. Soc.* **2005**, *127*, 6744–6751.
[30] L. Shi, V. D. Paoli, N. Rosenzweig, Z. Rosenzweig, *J. Am. Chem. Soc.* **2006**, *128*, 10378–10379.
[31] A. C. S. Samia, X. Chen, C. Burda, *J. Am. Chem. Soc.* **2003**, *125*, 15736–15737.
[32] H. Peng, L. Zhang, T. H. M. Kjallman, C. Soeller, J. Travas-Sejdik, *J. Am. Chem. Soc.* **2007**, *129*, 3048–3049.
[33] S. J. Chen, H. T. Chang, *Anal. Chem.* **2004**, *76*, 3727–3734.
[34] R. Wargnier, A. V. Baranov, V. G. Maslov, V. Stsiapura, M. Artemyev, M. Pluot, A. Sukhanova, I. Nabiev, *Nano Lett.* **2004**, *4*, 451–457.
[35] C. H. Fan, S. Wang, J. W. Hong, G. C. Bazan, K. W. Plaxco, A. J. Heeger, *Proc. Natl. Acad. Sci. USA* **2003**, *100*, 6297–6301.
[36] T. Huang, R. W. Murray, *Langmuir* **2002**, *18*, 7077–7081.
[37] E. Oh, M.-Y. Hong, D. Lee, S.-H. Nam, H. C. Yoon, H.-S. Kim, *J. Am. Chem. Soc.* **2005**, *127*, 3270–3271.
[38] L. Wang, R. Yan, Z. Huo, L. Wang, J. Zeng, J. Bao, X. Wang, Q. Peng, Y. Li, *Angew. Chem.* **2005**, *117*, 6208–6211; *Angew. Chem. Int. Ed.* **2005**, *44*, 6054–6057.
[39] L. Dyadyusha, H. Yin, S. Jaiswal, T. Brown, J. J. Baumberg, F. P. Booy, T. Melvin, *Chem. Commun.* **2005**, 3201–3203.
[40] I. Goldstein, C. Hollerman, J. Merrick, *Biochim. Biophys. Acta* **1965**, *97*, 68–76.
[41] C. Borrebaeck, B. Mattiasson, *Anal. Biochem.* **1980**, *107*, 446–450.
[42] D. A. Mann, M. Kanai, D. J. Maly, L. L. Kiessling, *J. Am. Chem. Soc.* **1998**, *120*, 10575–10582.
[43] T. Hasegawa, S. Kondoh, K. Matsuura, K. Kobayashi, *Macromolecules* **1999**, *32*, 6595–6603.
[44] D. M. Willard, L. L. Carillo, J. Jung, A. Van Orden, *Nano Lett.* **2001**, *1*, 469–474.
[45] H. Bittiger, H. P. Schnebli, *Concanavalin A as a Tool*, Wiley, London, **1976**.
[46] J. R. Lakowicz, *Principles of Fluorescence Spectroscopy*, 2nd ed., Plenum Press, New York, **1999**, p. 237.
[47] M. Gao, A. L. Rogach, A. Kornowski, S. Kirstein, A. Eychmuller, H. Mohwald, H. Weller, *J. Phys. Chem. B* **1998**, *102*, 8360–8363.
[48] B. Tang, H. L. Liang, K. H. Xu, Z. Mao, X. F. Shi, Z. Z. Chen, *Anal. Chim. Acta* **2005**, *554*, 31–36.
[49] G. Frens, *Nat. Phys. Sci.* **1973**, *241*, 20–22.

Received: November 28, 2007
Published online: March 3, 2008

